Available online at www.sciencedirect.com
SCIENCE DIRECT®
PHYSICS LETTERS A
ELSEVIER
Physics Letters A 309 (2003) 109–113
www.elsevier.com/locate/pla

Formation mechanism of alumina nanotube array

Y.F. Mei [a], X.L. Wu [a,*], X.F. Shao [a], G.S. Huang [a], G.G. Siu [b]

[a] *National Laboratory of Solid State Microstructures and Department of Physics, Nanjing University, Nanjing 210093, PR China*
[b] *Department of Physics and Materials Science, City University of Hong Kong, Kowloon, Hong Kong, PR China*

Received 16 June 2002; received in revised form 21 January 2003; accepted 21 January 2003

Communicated by A.R. Bishop

Abstract

Formation mechanism of alumina nanotubes and their array was analysed on the basis of voids in both anodic porous alumina membrane and the tube walls of alumina nanotubes. Circular, crack-like, and wheel-like voids were observed and considered to be responsible for the formation of aluminian nanotubes and their array. Based on microstructural observation of individual alumina nanotubes, the morphology of the tube wall filled with the voids was experimentally determined, which will help to understand the formation mechanism of alumina nanotubes. Our observations and analyses give further information on self-organized mechanism of anodic porous alumina membrane.

PACS: 85.42.+m; 82.65.Yh; 61.72.Qq

Keywords: Alumina; Nanotubes; Microstructure

Since the discovery of carbon nanotubes [1], which have various peculiar chemical and physical properties as well as potential applications in modern nanodevices, many investigations have focused on preparations, properties, and applications of other nanotubes and their arrays [2–5]. Among these investigations, the explorations of new fabrication methods have become a subject of a large number of studies. For example, using porous silicon or porous alumina membrane as a template, carbon nanotubes and their arrays may be formed by growing the carbon nanotubes in the pores of the template [6–8]. The pore ordering and diameter of the template determine the structures of the fabricated nanotubes and arrays. However, carbon nanotubes fabricated with such a template are usually packed each other and difficult to be separated. In the recent work [3], we obtained individual alumina nanotubes (ANTs) in terms of ordinary anodization of Si-based aluminum membrane. This investigation is expected to open fascinating possibilities for further chemical and physical explorations of nanostructures such as individual carbon nanotubes, nanowires, cylindrical capacitors, and nanocables, which are useful in future nanodevices. However, the ANT arrays have not yet been obtained and the formation mechanism of the ANTs is still unclear. Therefore, further work is needed to address these issues.

* Corresponding author.
E-mail address: hkxlwu@nju.edu.cn (X.L. Wu).

0375-9601/03/$ – see front matter
doi:10.1016/S0375-9601(03)00130-0

In this Letter, we report the formation processes of the ANTs and their arrays by transmission electron microscope (TEM) observations on the alumina membranes. Two types of aluminum oxide membranes were obtained, which were called as porous and barrier types of alumina membranes [9,10], respectively. For this porous type of alumina membranes, we found that if additional anodization is carried out under a pulse voltage before the membrane will be detached from the Si mother skeleton, the combination and separation of the ANTs can easily be controlled. In addition, we found that the voids in the membrane not only appear at triple points between cell grains but also exist elsewhere such as in the tube walls of the ANTs. By analyzing the morphology of the tube walls, a model concerning evolution of the voids in the porous alumina membrane was presented to describe this formation mechanism of the ANTs and their arrays.

Individual ANTs can be obtained on the basis of previous fabrication conditions [3]. In our current experiments, p-type $\langle 100 \rangle$-oriented silicon wafers with a resistivity of 5 Ω cm were used. A layer of Al film with a thickness of 440 nm and a purity of 99.99% was deposited onto the Si wafer by electron beam evaporation (we call it as Al/Si system). Anodization with a platinum plate as a cathode and the Al/Si system as anode was carried out in 15 wt.% sulfuric acid under a constant dc voltage of 40 V. The temperature of the electrolyte was set at room temperature (about 27 °C). The anodization process can be controlled through the current-time curve. If the anodization was carried out until the anodic porous alumina membrane was detached from the silicon substrate, we call this process after normal method. If the anodization was stopped (turning off the current) at the moment when the silicon wafer just starts to be anodised and the Al membrane has completely been anodised, and subsequent anodization was continued for a short time (1 s) by pulse voltage (the maximum voltage is 40 V) instead of dc voltage, we call this process after abnormal method. The abnormal method can also completely detach the anodic porous alumina membrane from the silicon substrate. The normal method is a traditional method for fabricating the porous alumina membrane. The abnormal method is further anodization of the porous alumina membrane under a pulse voltage. After anodized with the normal or abnormal method, the porous alumina membranes were immersed into a 5 wt.% phosphoric acid solution for several minutes and followed by TEM observations on a Hitachi H-800-NA microscope operated at 200 keV.

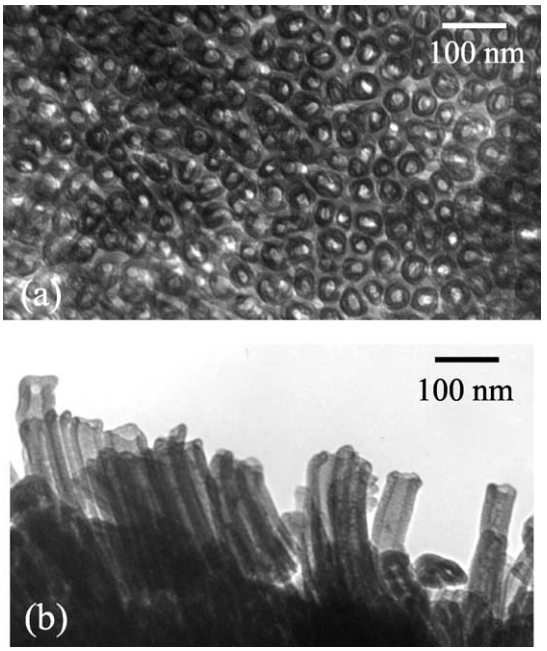

Fig. 1. (a) Planar and (b) cross-sectional TEM images of the isolated ANT array.

The ANT array can be obtained by the abnormal method. The ANTs are packed each other. Figs. 1(a) and (b) show the planar and cross-sectional TEM images of the ANT array, respectively. From this figure, we can estimate the mean outer and inner diameters of the isolated ANT to be about 40 and 20 nm. To reveal the formation process of the ANT array, we fabricated the sample anodized with the normal method and then immersed it into 5 wt.% phosphoric acid solution for several minutes. A TEM image of the obtained porous alumina membrane is shown in Fig. 2(a). The nanopore arrangement is uniform and ordered. The mean diameter of nanopores is about 20 nm. With increasing the immersed time, circular voids appear at triple points between cell grains, as shown in Fig. 2(b). In addition, crack-like voids can also be observed in the porous alumina membrane (see the arrow). From the morphology of crack-like voids, we may infer that they arise from originally circular voids. Using the abnormal method and subsequent immersion into 5 wt.% phosphoric

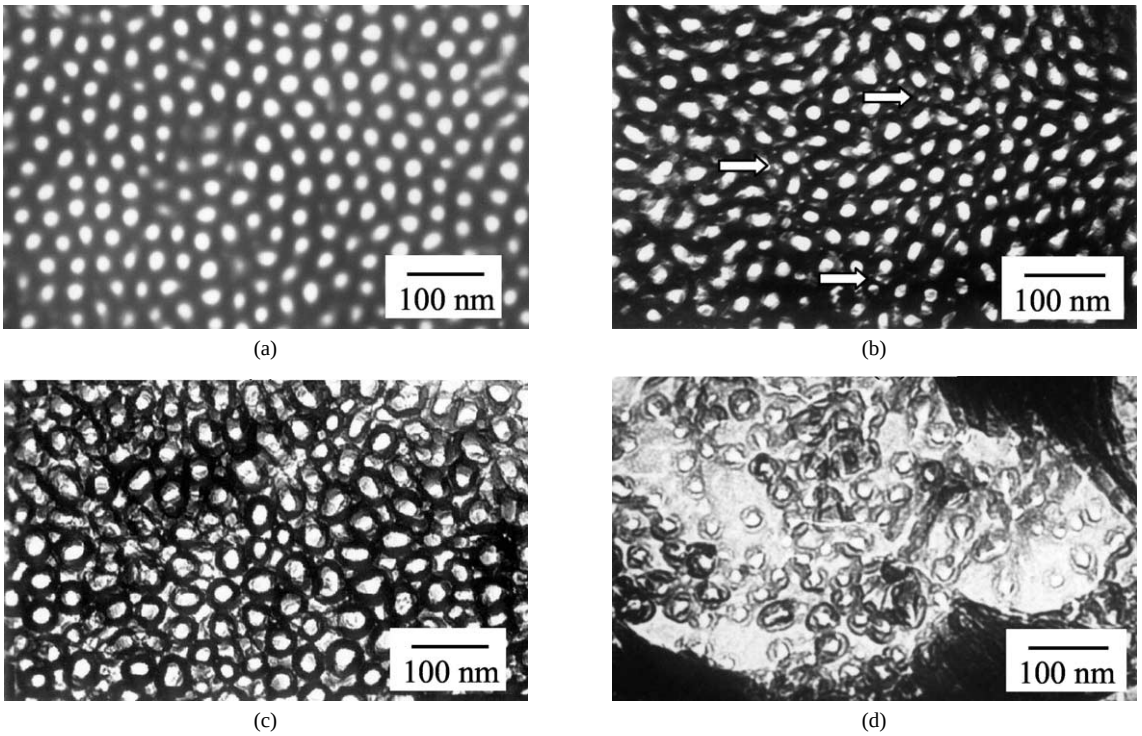

Fig. 2. Two TEM images of the porous alumina membrane formed with (a) normal method and then immersion into 5 wt.% phosphoric acid solution for several minutes and (b) further prolonging the immersed time. Two TEM images of the ANT array formed with (c) abnormal method and then immersion into 5 wt.% phosphoric acid solution for several minutes and (d) further prolonging the immersed time.

acid solution for several minutes, we can obtain the ANT array, as shown in Fig. 2(c). It can be seen that the voids have evolved from circular and crack-like shapes to "cracks" around the isolated ANTs. It is the "cracks" that lead to the formation of the ANTs and their array. With further prolonging the immersed time in the phosphoric acid solution, wheel-like voids can be observed in the tube walls of the isolated ANTs (see Fig. 2(d)). These observations indicate that the voids play an important role in the formation of the ANT array.

Shown in Fig. 3(a) is a TEM image of single ANT. We can see that the outer wall of the ANT is not smooth, displaying a large surface fluctuation. A row of voids exists in the tube walls (by the arrow). Obviously, the wheel-like voids, which are observed in Fig. 2(d), are a top projection of this row of voids in the tube wall. This image clearly displays that the region between the inner and outer walls consists of the voids. In addition, we found that the observed voids will enlarge or merge under electron beam irradiation to form bigger voids along the tube wall. This result implies that further dissolution of the hydrated oxide (e.g., $Al(OH)_3$ or AlOOH) in the tube wall takes place. This process cannot be due to lattice distortion of the alumina membrane caused by electron beam irradiation. Obviously, if the tube wall is a continuum without the voids, as proposed in the electric-assisted dissolution model [11], electron beam irradiation should not lead to enlargement of the voids in the tube wall. In fact, this dissolution process gives many clues for seeking the growth mechanism of self-organized cell grains (one cell corresponds to an ANT). In the previous literature [12,13], some authors have proposed that the voids are only located at triple points between cell grains in the porous alumina membrane, because the low volume of metal per unit interfacial area subtending the interface adjacent to the apex has a larger ability to accommodate vacancies than do regions removed from apex [13]. Although this model cannot completely explain our current experimental results, a slightly modified model could

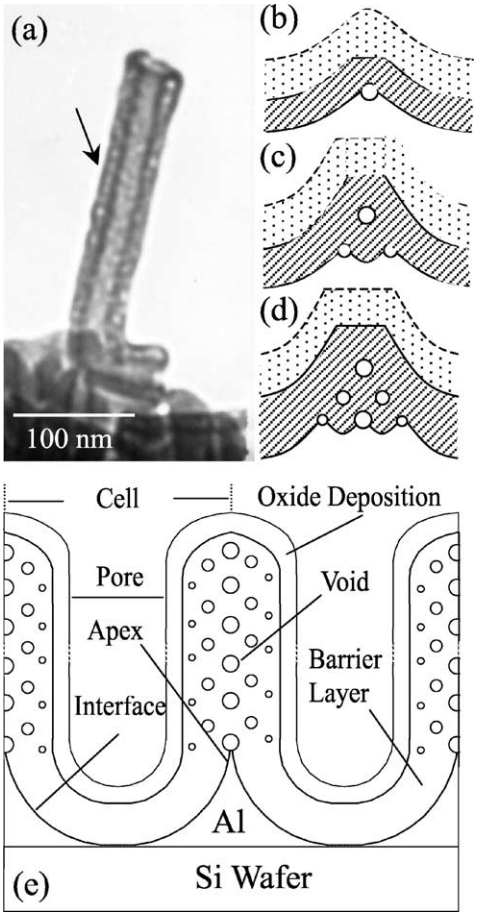

Fig. 3. (a) A TEM image of an individual ANT. The outer wall of the ANT is not smooth and many voids can clearly be observed in the tube wall (by the allow). (b)–(e) A series of schematic diagrams for the formation and distribution of the voids during the formation of the ANT array. Note that the relative dimensions are not to scale.

be contrived, as shown in Fig. 3(b)–(e). When a void is detached from the apex of protrusion at the intersection of three cell grain boundaries (Fig. 3(b)), three apexes are simultaneously formed. The three apexes should be easier to accommodate vacancies than other regions at the interface between metal and the oxide. Therefore, new three voids will nucleate in the barrier layer and then grow due to the condensation of cation and/or metal vacancies (Fig. 3(c)). Similar process proceeds to form more apexes and thus more voids nucleate and grow (Fig. 3(d)). This situation lasts, similar to the case described by Macdonald [13]. Finally, we may obtain the distribution of the voids during the formation of the ANT array, as shown in Fig. 3(e). A sharp feature of this model is that with thickening the alumina film, the voids begin growth at the triple points and then are gradually full of whole grain boundaries. Therefore, the voids with the largest sizes are located at the triple points between cell grains. The voids with small sizes appear in the inner diameter of the cell grain. When a pulse voltage is applied to the porous alumina membrane, the tensile stress changed abruptly will split the junctions between the voids and thus lead to the interlaced cleavages of the cells. As a result, the ANTs and their array are formed.

In conclusion, the formation mechanism of the ANTs and their array has been discussed on the basis of evolution of the voids in the porous alumina membrane. A modified model is presented to describe this formation process. We have disclosed that the voids in the cell boundaries are responsible for growth of the cracks between alumina cells and thus formation of the ANT array. The morphology of individual ANT observed is consistent with our analyses. The formation mechanism of ANT array and the morphology of individual ANTs give important information for self-organized mechanism of the porous alumina membrane.

Acknowledgements

This work was supported by the Grants (Nos. 10225416 and BK2002077) from the Natural Science Foundations of China and JiangSu province. Partial support was also from the special funds for Major State Basic Research Project No. G2001CB3095 of China and the Trans-Century Training Programme Foundation for the Talents by the State Education Commission.

References

[1] S. Iijima, Nature 354 (1991) 56.
[2] M.E. Spahr, P. Bitterli, R. Nesper, M. Müller, F. Krumeich, H.U. Nissen, Angew. Chem. Int. Ed. 14 (1998) 3160.
[3] L. Pu, X.M. Bao, J.P. Zou, D. Feng, Angew. Chem. Int. Ed. 40 (2001) 1490.
[4] R. Parthasarathy, C.R. Martin, Nature 369 (1994) 298.
[5] T. Kyotani, L. Tsai, A. Tomita, Chem. Mater. 8 (1996) 2190.

[6] S.J. Tans, A.R.M. Verschueren, C. Dekker, Nature (London) 393 (1998) 48.
[7] J. Li, C. Papadopoulos, J.M. Xu, Nature (London) 402 (1999) 253.
[8] J. Li, C. Papadopoulos, J.M. Xu, Appl. Phys. Lett. 75 (1999) 367.
[9] G.E. Thompson, Thin Solid Films 297 (1997) 192.
[10] R.S. Alwitt, C.K. Dyer, J. Electrochem. Soc. 129 (1982) 711.
[11] J.P. O'Sullivan, G.C. Wood, Proc. R. Soc. London A 317 (1970) 511.
[12] S. Ono, H. Ichinose, N. Masuko, J. Electrochem. Soc. 138 (1991) 3705.
[13] D.D. Macdonald, J. Electrochem. Soc. 140 (1993) L27.